Shear Thinning in Ternary Bicontinuous and Water-in-Oil Microemulsions

Mark R. Anklam
TRI/Princeton and Dept. of Chemical Engineering, Princeton University, Princeton, NJ 08544

Robert K. Prud'homme
Dept. of Chemical Engineering, Princeton University, Princeton, NJ 08544

Gregory G. Warr
Dept. of Chemical Engineering, Princeton University, Princeton, NJ 08544, and Div. of Physical and Theoretical Chemistry, The University of Sydney, Sydney, NSW, 2006, Australia

Shear thinning of ternary microemulsions of didodecyldimethylammonium bromide (DDAB), water, and dodecane in the range 10^3 to 10^6 s^{-1} is documented over a wide range of compositions. A marked transition in the characteristic shear rate is observed accompanying the structural transition from bicontinuous to water-in-oil (w/o) droplets as previously reported from diffusion and small-angle scattering techniques. Results in the w/o region are consistent with those for a dispersion of hard spheres. The shear thinning of the bicontinuous structure, however, occurs at much higher shear rates, implying a shorter time and length scale for disruption of the equilibrium liquid structure by the flow field.

Introduction

In this study rheology is used to probe the dynamics and structure of ternary microemulsions comprising dodecane, water, and the surfactant didodecyldimethylammonium bromide (DDAB). Non-Newtonian flow in micellar solutions has been documented extensively (Rehage and Hoffmann, 1988; Hoffmann et al., 1992), and there are scattered studies in which shear thinning of microemulsions has been reported or inferred (Thurston et al., 1979; Quemada and Langevin, 1985; Bennett et al., 1981). We have previously examined the shear rheology of DDAB/dodecane/water microemulsions, and found them to be Newtonian at shear rates between 0.3 and several thousand reciprocal seconds (Chen, 1992; Chen and Warr, 1992). Investigations with a constant shear stress device confirmed the absence of a yield stress. In this work we have extended the range of shear rates up to 10^6 s^{-1}, and document the shear rates at which shear thinning occurs as a function of composition and hence microemulsion structure for the first time.

DDAB forms microemulsions with a variety of hydrocarbons over a wide range of compositions (Chen et al. 1984; Blum et al., 1985; Barnes et al., 1988a, b), exhibiting both bicontinuous and water-in-oil (w/o) droplet structures depending on composition. As DDAB is insoluble in both water and alkanes, it is exclusively present at the oil/water interface within the microemulsion. Unlike many microemulsions, DDAB systems thus do not exhibit normal or inverse micelle phases that can swell with addition of an immiscible second solvent. Instead substantial amounts of both oil and water are required for microemulsion stability. The one phase microemulsion region for DDAB + oil + water is shown on a ternary phase diagram in Figure 1. The structure of these microemulsions has been well studied by numerous techniques (Chen et al., 1984; Blum et al., 1985; Barnes et al., 1988a,b). The generally accepted picture is of interconnected water tubes coated with an oriented monolayer of surfactant and dispersed in an oil continuum. The water channels meet or intersect at nodes so that the liquid structure resembles a solvent-swollen cross-linked polymer.

The most detailed model of these structures, known as the DOC-cylinders model, regards the nodes as surfactant-coated water spheres (Barnes et al., 1988a,b; Hyde et al., 1989). Neighboring spheres are connected by cylinders of surfactant-coated water so that each node has a coordination number of con-

Correspondence concerning this article should be addressed to G. G. Warr.

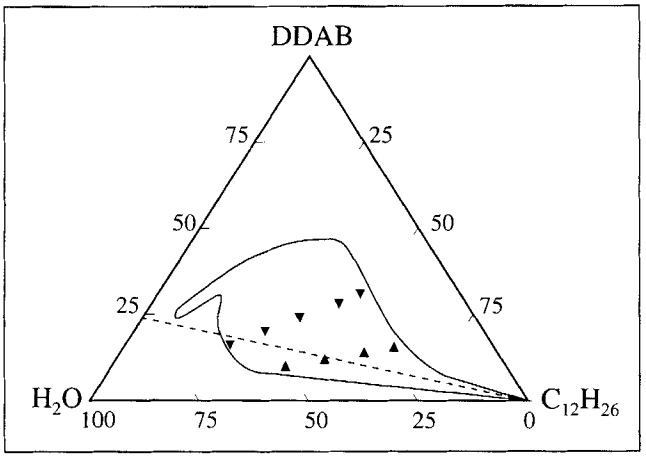

Figure 1. Partial ternary phase diagram of DDAB/dodecane/water microemulsions showing the boundary of the microemulsion phase and the compositions of samples studied.

The dashed line is the "percolation line," indicating the locus of compositions where the microemulsions transform from bicontinuous (above) to water-in-oil (below).

nected neighbors. The combination of spheres and cylinders provides a convenient geometrical basis for modeling the structure: this relates oil and water volume fractions and interfacial area (surfactant concentration) to the coordination number and number density of nodes.

The other major influence on the microemulsion structure is the preferred curvature of the oil/water interface within the microemulsion. This is determined by the structure of the surfactant packed at the interface, and on the anisotropy of the lateral interactions between neighboring head groups and alkyl chains on either side of the interface.

In general the observed sequence is that as water is added to a particular DDAB microemulsion the increasing water volume fraction and constant interfacial area combine to decrease the surface/volume ratio. The net effect of this is to increase the fraction of water in droplets at the expense of cylinders, hence decreasing the coordination number of the droplets. As further water is added the system eventually undergoes a reverse percolation from a bicontinuous structure to discrete w/o droplets. This feature mirrors the experimental observation of an abrupt decrease in conductivity and in the diffusion of water (Chen et al., 1984).

Much less is known about the dynamics of microemulsions. It might be expected that the gross structural changes in the liquid with different water content would be reflected in the rheology through both the viscosity and the shear thinning behavior. We have previously shown that structural transformations are only apparent in microemulsion viscosity at low shear at low volume fractions of oil. Once the volume fractions of oil and water become comparable, excluded volume effects dominate the viscosity. Microemulsions were also found to be Newtonian up to very high shear rates, even compared with micellar systems, indicating a short structural relaxation time for these liquids (Chen and Warr, 1992). Extension of the viscosity measurements into the shear thinning regime and even to the limiting high shear viscosity in some cases is presented below.

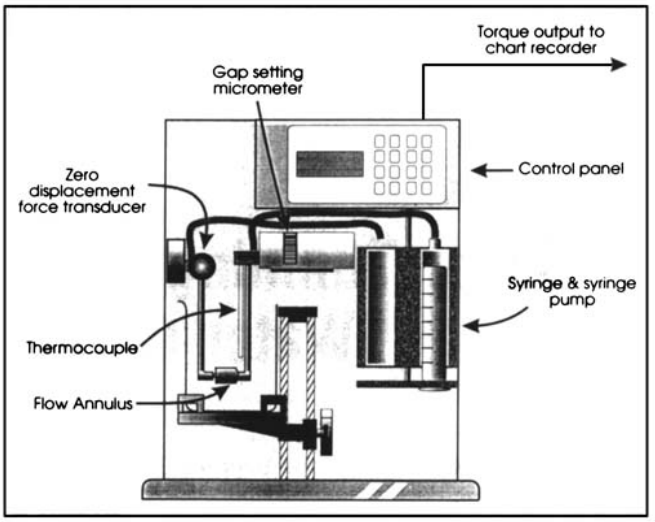

(a)

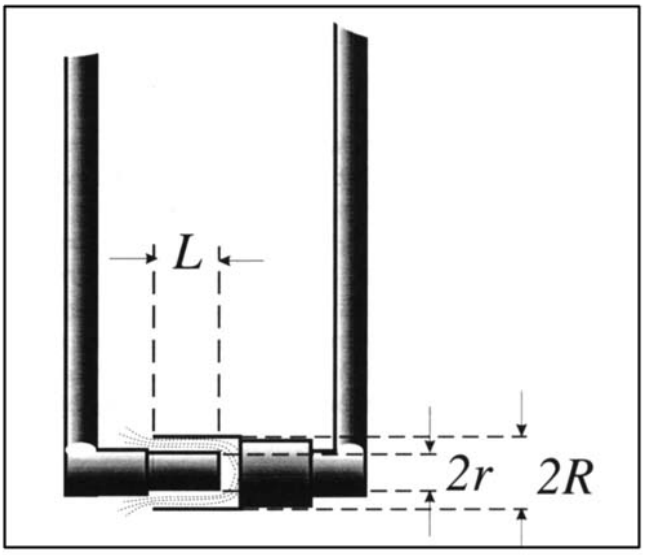

(b)

Figure 2. (a) Rheometrics RFX in shear flow configuration; (b) expanded view of the annular flow geometry in the RFX.

Experimental Procedures

Viscosities were measured using the Rheometrics RFX, in the configuration shown in Figure 2. The RFX is designed primarily for investigating elongational flow in an opposing nozzle geometry, but it can also be used to study shear flows, and is particularly suited to high shear rates. In the shear configuration, the RFX operates using annular flow of liquid through a cylinder and around a second cylinder or pin inserted into the larger cylinder. The liquid is pumped from an external reservoir by a syringe pump. The Poiseuille flow developed in the annulus at a particular flow rate generates a wall shear stress at the inner and outer cylinders and a corresponding wall shear rate. The stress on the inner cylinder is measured from the torque on a zero displacement force transducer, which maintains the position of the inner plug. Wall shear rate can

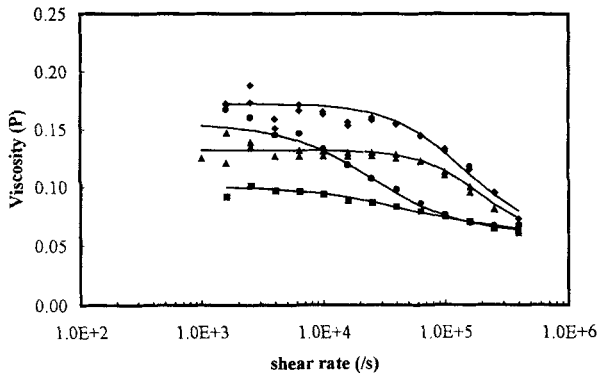

Figure 3. Variation of viscosity with shear rate for microemulsions along the s:o 20:80 water dilution line.

♦ 22 wt. %; ▲ 30 wt. %; ■ 40 wt. %; ● 50 wt. %. Solid lines calculated from Eq. 2.

be determined from the total flow rate and geometry of the cell using

$$\dot{\gamma}_{\text{wall}} = \frac{6Q}{\pi(R+r)h^2} \tag{1}$$

where Q is the volumetric flow rate, R the outer cylinder radius, r the inner cylinder radius, and $h = R - r$ is the size of the gap. The viscosity is then obtained from a simple ratio of the shear stress to the shear rate at the wall.

The RFX is modified to allow accurate centering of the two cylinders used. The position of the inner cylinder (pin) is controlled by micrometers allowing adjustment in the vertical and horizontal planes (Figure 2). The position of the inner cylinder is sensed by two linear strain gauges, and contact between inner and outer cylinders is registered by the zero displacement force transducer. By measuring the contact positions against opposite walls the pin can be centered in the outer cylinder.

In order to avoid cavitation, experiments were generally run with liquid being expelled from the syringe pump, rather than being sucked into the syringes. In those experiments where the flow direction was reversed the measured viscosities were unaffected. Pumping the liquid into the cell generates an "end effect" due to the hydrodynamic pressure of the liquid on the end of the pin. This effect is accounted for by measuring the apparent viscosity at different insertion distances. In this work we found no dependence of measured viscosity on pin length, hence the end effect must be negligible. Previous work using this apparatus has shown that both water and a range of light hydrocarbons are Newtonian at shear rates as high as 7×10^5 s^{-1} (Krieger, 1992).

The range of shear rates examined overlaps slightly with previous results for these microemulsions at lower shear rates investigated using Couette and cone-and-plate viscometers (Chen and Warr, 1992). These are compared with the present results where appropriate.

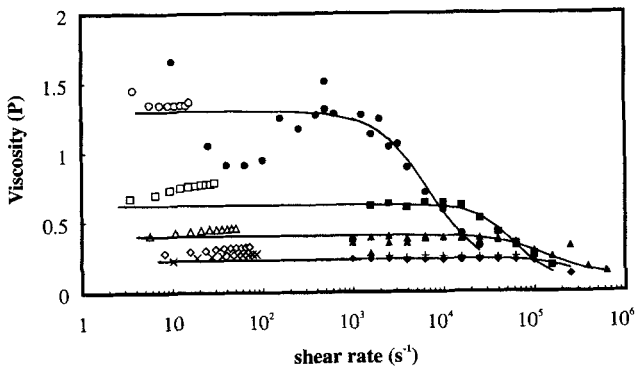

Figure 4. Variation of viscosity with shear rate for microemulsions along the s:o 40:60 water dilution lines.

× + 22 wt. %; ◇ ♦ 30 wt. %; △ ▲ 40 wt %; ■ ⧈ 50 wt. %; ○ ● 60 wt %. Open symbols denote Couette measurements (Chen and Warr, 1992) and closed symbol the present work. Solid lines calculated from Eq. 2.

Results

Viscosities of microemulsions were measured as a function of shear rate for compositions along two water dilution lines. Surfactant:oil (w/w) ratios were held constant at 20:80 and 40:60. The compositions studied are indicated on a ternary phase diagram showing the phase boundary of the microemulsion in Figure 1. The dashed line in Figure 1 shows the "percolation line," indicating the locus of compositions where the microemulsions transform from bicontinuous (above) to water-in-oil (below). As can be seen, both the 20:80 and 40:60 compositions span bicontinuous and water-in-oil (w/o) structures for this microemulsion.

Viscosities as a function of shear rate for microemulsions along the s:o = 20:80 and 40:60 dilution lines are shown in Figures 3 and 4. Also shown in Figure 4 are the low shear results from previous work (Chen and Warr, 1992). All microemulsions studied exhibited shear thinning at sufficiently high shear rates. For most microemulsions this was above $10^4 s^{-1}$, and many systems had not reached a limiting high shear rate viscosity even at 10^6 s^{-1}.

The shear thinning behavior shown in Figures 3 and 4 can be described empirically by the Cross equation (Cross, 1965)

$$\frac{\eta - \eta_\infty}{\eta_0 - \eta_\infty} = \frac{1}{1 + \left(\frac{\dot{\gamma}}{\dot{\gamma}_c}\right)^n} \tag{2}$$

where η_0 is the zero or limiting low shear viscosity, η_∞ the limiting high shear viscosity, γ_c is a critical shear rate, and n is a positive number that describes the steepness of the shear thinning. At the critical shear rate, η is midway between η_∞ and η_0, and hence provides a convenient measure of the relaxation time for structural fluctuations in the liquid.

The agreement between results from the RFX and earlier Couette cell work is excellent at low shear rates for the 40:60 mixtures. Low shear rate viscosities from both techniques are compared in Figure 5. Also shown are the limiting high shear viscosities obtained in this study by fitting the data shown in Figure 4 to Eq. 2.

The agreement with earlier results is less satisfactory for the 20:80 dilution line. Figure 6 compares the low shear viscosity determined in this and previous work. Limiting high shear viscosities obtained from fitting the data of Figure 3 to Eq. 2 are also shown. The viscosities agree passably well, in fact as

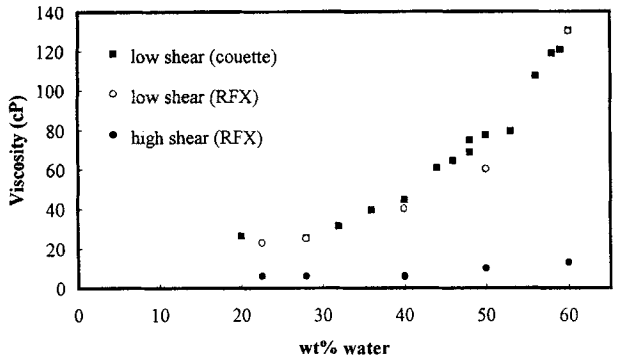

Figure 5. Limiting low (○) and high (●) shear rate viscosities for microemulsions along the s:o 40:60 water dilution line.

Also shown are results obtained previously using a Couette rheometer (■) (Chen and Warr, 1992).

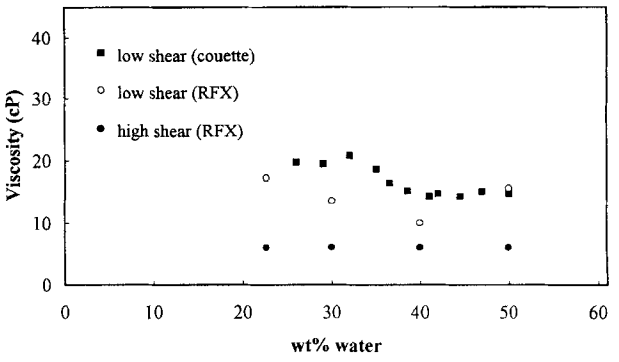

Figure 6. Limiting low (○) and high (●) shear rate viscosities for microemulsions along the s:o 20:80 water dilution line.

Also shown are results obtained previously using a Couette rheometer (■) (Chen and Warr, 1992).

well as for the s:o = 40:60 line in absolute units, but in relative terms there is sufficient discrepancy that trends in the low shear viscosity are masked by experimental scatter.

The observed shear thinning could arise from viscous heating of the microemulsions at high shear rates. This is unlikely given the strong dependence of critical shear rate on composition, indicating the effect of microemulsion structure on its rheology. Temperature profiles for fluids undergoing Poiseulle flow can be determined from their heat capacity and the temperature dependence of their viscosity and thermal conductivity (Winter, 1977). Using our best estimates for these parameters for the DDAB microemulsions studied, heating by the order of only 1°C is anticipated at $10^6\ s^{-1}$ (Radlinska et al., 1989; *CRC Handbook*). This is insufficient to cause the observed shear thinning behavior in which the viscosity changes by a factor of between 2 and 10.

Discussion

The remarkable observation for these microemulsions is that the critical shear rate of the bicontinuous microemulsions is up to an order of magnitude greater than for those having a w/o structure (Figure 1). For both o:s = 60:40 and 80:20, the critical shear rate of these microemulsions decreases with addition of water and the accompanying structural transformation from bicontinuous to water droplets in oil. As Table 1 shows, the change in critical shear rate seems to be a quite abrupt companion of the structural transformation. Also, γ_c remains constant within experimental uncertainty along either dilution line as long as the bicontinuous network structure is maintained, and this indicates a different mechanism of structural relaxation within the two domains of the single-phase region. Despite the large changes in relaxation times, however, the steepness of the shear thinning depends very little on composition.

There is a large body of work on the rheology of monodisperse hard sphere suspension (de Kruif et al., 1985; van Megen et al, 1987; van Blaaderen et al., 1992; Cohen and de Schepper, 1992), and this is the simplest model for microemulsions with w/o structure. In such dispersions shear thinning is expected to occur when the viscous forces and Brownian forces are comparable. Alternatively, this can be viewed in terms of characteristic times for viscous and Brownian motions. The timescale for Brownian relaxation of a droplet of radius r_{drop} is r_{drop}^2/D, where D is the self-diffusion coefficient, and the shear timescale is given by $1/\dot{\gamma}$. This leads to a Peclet number defined as

$$Pe = \frac{\dot{\gamma}\, r_{drop}^2}{D}. \tag{3}$$

The Peclet number increases with shear rate, so that low Pe indicates that liquid structure is dominated by Brownian motion, whereas large Pe indicates a liquid where viscous interactions are dominant. At Peclet numbers of order one, the

Table 1. Critical Shear Rates, γ_c, and Relaxation Times, τ, for DDAB/Dodecane/Water Microemulsions

	o:s = 80:20				o:s = 60:40			
Wt% Water	γ_c/s^{-1}	Pe_c	τ/s	n	γ_c/s^{-1}	Pe_c	τ/s	n
22.6	1.4×10^5		7×10^{-6}	1.5	1.4×10^5		7×10^{-6}	1.5
30.0	1.4×10^5		7×10^{-6}	1.5	1.4×10^5		7×10^{-6}	1.5
40.0	5×10^4	0.22	2×10^{-5}	1	1.4×10^5		7×10^{-6}	1.5
50.0	2.5×10^4	0.17	4×10^{-5}	1.2	6×10^4	0.52	1.7×10^{-5}	2
60.0					7×10^3	0.09	1.4×10^{-4}	1.5

Note: Microemulsions with compositions above the dashed line are bicontinuous, and those below are w/o droplets.

viscous forces thus influence liquid structure significantly, and non-Newtonian behavior is expected. DDAB microemulsions have been extensively studied, and the droplet radius in the w/o region is known from small-angle scattering (Barnes et al., 1988a). Self-diffusion coefficients of the oil, water, and surfactant components of the microemulsions have also been measured, and in the w/o region we take this to be equal to the droplet diffusion coefficients (Blum et al., 1985). At compositions where diffusion constants have not been measured, we have used the approximate relationship between viscosity and diffusion coefficient of a dispersion of spheres at volume fractions 1 and 2: $\eta_1/\eta_2 = D_2/D_1$ (van Blaaderen et al., 1992; Cohen and de Schepper, 1992). Peclet numbers calculated at $\dot{\gamma}_c$ using these parameters are listed in Table 1, and it can be seen that shear thinning indeed occurs when Pe is of order 1, although always below 1. Previous studies of hard sphere dispersions also report shear thinning at Peclet numbers somewhat less than 1, so our results in the w/o region are consistent with a microemulsion comprising droplets that behave as hard spheres. As with the low shear viscosities, it is not necessary to include droplet coalescence or deformability, or "softness" of interactions due to the surfactant layer to describe the data at this semiquantitative level (Chen and Warr, 1992).

The Peclet number for spherical dispersions is more commonly represented as

$$\mathrm{Pe} = \frac{6\pi\eta_s \dot{\gamma} r_{\mathrm{drop}}^3}{kT} \tag{4}$$

where η_s is the viscosity of the solvent, in this case dodecane; 1.35 cp. This form is obtained by using a Stokes' law representation of the sphere diffusion coefficient, and corresponds to infinite dilution of droplets. In might also be regarded as the diffusion of a droplet within a coordination cage of neighboring spheres: the short time limit of the diffusion coefficient, as distinct from the long time value obtained from PGFT-NMR (Blum et al., 1985). Experiments on hard sphere systems and theoretical analysis have both shown a dependence of the short time diffusion coefficient on volume fraction of dispersed phase, so this definition of the Peclet number is not strictly appropriate for concentrated dispersions. However, it, too, gives Peclet numbers of order 1 for the w/o DDAB microemulsions examined here.

In the bicontinuous region the shorter relaxation time suggests that a different structural reorganization mechanism must operate. The relaxation times in these systems are much shorter than we estimated for a diffusion-limited droplet coalescence mechanism (Chen and Warr, 1992), which actually gives more reasonable agreement with results in the w/o region. Possible relaxation mechanisms fall into two classes: those involving surfactant exchange from the oil/water interface, and those involving structural fluctuations at constant interfacial composition and area.

Surfactant exchange is known to be important in the dynamics of aqueous micelles, involving both exchange of individual monomers and also dissolution/aggregation processes (Aniansson et al., 1976). In four- and five-component microemulsions (water, oil, surfactant, cosurfactant, electrolyte), ultrasonic absorbance measurements in the range 3–100 MHz show relaxations that have also been attributed to exchange processes (Hirsch et al., 1984; Lange et al., 1980). Middle phase (bicontinuous) microemulsions have relaxation frequencies of order 10 MHz, which is significantly faster than that responsible for the observed shear thinning in the present work. This disparity of timescale could be explained by the low solubility of the surfactant in both solvents. As the adsorption of surfactant is essentially diffusion limited (Morgan et al., 1992), low solubility implies a considerably slower rate of surfactant desorption from the interface than, say, for the dodecyl sulfate ion (Lang et al., 1980), and is a possible origin for the observed relaxation.

Structural rearrangement without surfactant exchange could arise from the easing of constant area or curvature constraints employed in the DOC and other geometrical models (Barnes et al., 1988b; Hyde et al., 1989; Chen et al., 1988). Bending energy parameterizations would be one way of introducing variable curvature (Chevalier and Zemb, 1990). A reorganization mechanism previously proposed for bicontinuous microemulsions (Chen and Warr, 1992) and sponge phase (Snabre and Porte, 1992) involves the shrinking or necking of conduits, and then their pinching off. The relaxation time for the shrinking of conduits, τ_s, has been estimated as (Snabre and Porte 1992)

$$\tau_s = \frac{6\pi\eta_s d^3}{kT}. \tag{5}$$

where η_s is the solvent viscosity, d the conduit diameter, and k is the Boltzmann constant. An activation barrier associated with the local fusion of membranes has also been postulated; however, for the low interfacial tensions in a microemulsion we will neglect this. Structural and phase equilibria studies of these microemulsions have indicated a dependence of optimal curvature, and hence sphere and conduit radius, on composition (Hyde et al., 1989; Chen, 1992). For DDAB with dodecane, conduit radii lie between 10 and 50 Å, increasing with increasing water content. Using these values in Eq. 5 gives relaxation times of 1.4×10^{-1} to 2×10^{-4} s, or critical shear rates of 7×10^{5} to 6×10^{3} s^{-1}.

Calculated values for γ_c span the observed values obtained by fitting the shear rate dependent viscosities. This not only suggests small values for any activation energy of membrane fusion as anticipated, but also supports the proposed necking mechanism for shear thinning. This leads us to conclude that shear thinning is due to a structural rearrangement of the bicontinuous network rather than surfactant exchange.

Both bicontinuous and w/o microemulsions exhibit a peak in their small-angle scattering at a characteristic wave vector corresponding to a particular correlation distance in the liquid, D^* (Barnes et al., 1988a,b). In w/o systems this depends on interparticle distance, but in a random bicontinuous medium the identification of a characteristic distance is less clear. In the DOC model, D^* approximates the distance between neighboring (connected) droplets, which is between 200 and 400 Å in the present system. In a dynamic model the conduits fluctuate much faster than the diffusive motions of droplets, so that even when viscous forces are sufficient to affect droplet diffusion in w/o systems, the equilibrium structure in the bicontinuous state is essentially unperturbed. Shear thinning only occurs at much higher shear rates, comparable with the conduit fluctuation rates.

This mechanism implies a gradual breaking of interconnections along the shear gradient direction with increasing shear

rate, leading to a layered high shear structure. It is not evident to what extent the interconnected cylinder structure within these layers will reorganize into true lamellae or will retain water interpenetration. Probably the retention of in-plane structure depends on the shear rate: with increasing shear rate, progressively smaller structures are perturbed, so that the thickness of layers in the shear gradient direction is reduced. Eventually this length scale must become comparable with the radius of curvature of the surfactant film, at which point even droplets within the w/o region may be disrupted. At this point a swollen lamellar phase, aligned in the flow and vorticity directions, would be expected.

Some support for this is adduced from the observed limiting high shear viscosities of these systems (Figures 5 and 6). It can be seen here that η_∞ attains a constant value of approximately 6 cp. This viscosity is much lower than the measured limiting low shear viscosities, and is independent of composition, which might be expected for a sliding layer structure. Experimental conditions necessary for attainment of such high shear rates prevented any examination of the liquid structure under flow, which might resolve the mechanism of liquid reorganization.

Conclusion

The shear thinning behavior of three-component microemulsions with well-characterized microstructures have been examined as a function of composition. All bicontinuous microemulsions were observed to shear thin at extremely high shear rates, and this is interpreted in terms of fluctuations of conduits that make up the bicontinuous structure. As water is added and the structure becomes disconnected and eventually forms discrete water droplets, a marked reduction in critical shear rate occurs, signaling a change in the relaxation mechanism. In the w/o region, both the low shear viscosities (Chen and Warr, 1992) and the shear thinning behavior are adequately described in terms of hard sphere dispersions.

A lamellar high shear structure was inferred from the relaxation mechanism, and found to be consistent with observed high shear limiting viscosities.

Acknowledgment

This work was supported by the Australian Research Council and the University of Sydney through its Special Studies Programme. We wish to thank Dr. Paul Mode of Rheometrics for the use of the RFX and for his assistance with the experiments.

Literature Cited

Aniansson, E. A. G., S. N. Wall, M. Almgren, H. Hoffmann, I. Kielman, W. Ulbricht, R. Zana, J. Lang, and C. Tondre, "Theory of the Kinetics of Micellar Equilibria and Quantitative Interpretation of Chemical Relaxation Studies of Micellar Solutions of Ionic Surfactants," *J. Phys. Chem.*, **80**, 905 (1976).

Barnes, I. S., S. T. Hyde, B. W. Ninham, P.-J. Derian, M. Drifford, G. G. Warr, and T. N. Zemb, "The Disordered Open Connected Model of Microemulsions," *Prog. Colloid Poly. Sci.*, **76**, 90 (1988a).

Barnes, I. S., S. T. Hyde, B. W. Ninham, P.-J. Derian, M. Drifford, and T. N. Zemb, "Small-Angle X-Ray Scattering from Microemulsions Determines Microstructure," *J. Phys. Chem.*, **92**, 2286 (1988b).

Bennett, K. E., H. T. Davis, C. W. Macosko, and L. E. Scriven, "Microemulsion Rheology: Newtonian and Non-Newtonian Regimes," Paper No. SPE-10061, presented at the SPE 56th Annual Technical Conference and Exhibition, San Antonio, TX, (Oct. 5-7, 1981).

Blum, F. D., S. Pickup, B. Ninham, S. J., Chen, and D. F. Evans, "Structure and Dynamics in Three-Component Microemulsions," *J. Phys. Chem.*, **89**, 711 (1985).

Chen, C.-M., "Rheology of Ternary Microemulsions and Cubic Phases," MS Thesis, Univ. of Sydney (1992).

Chen, C.-M., and G. G., Warr, "Rheology of Ternary Microemulsions," *J. Phys. Chem.*, **96**, 9492 (1992).

Chen, S. J., D. F. Evans, and B. W. Ninham, "Properties and Structure of Three-Component Ionic Microemulsions," *J. Phys. Chem.*, **88**, 1631 (1984).

Chen, V., G. G. Warr, D. F. Evans, and F. G. Prendergast, "Curvature and Geometric Constraints as Determinants of Microemulsion Structure: Evidence from Fluorescence Anisotropy Measurements," *J. Phys. Chem.*, **92**, 768 (1988).

Chevalier, Y., and T. N. Zemb, "Structure of Micelles and Microemulsions," *Rep. Prog. Phys.*, **53**, 279 (1990).

Cohen, E. D. G., and I. M. de Schepper, "Transport Properties of Concentrated Colloidal Suspensions," *Slow Dynamics in Condensed Matter: Proc. Tohwa Univ. Int. and Symp.*, Fukuoka, Japan (1991); *AIP Conf. Proc.*, **256**, 359 (1992).

CRC Handbook of Chemistry and Physics, 60th ed., CRC Press, Boca Raton, FL (1980).

Cross, M. M., "Rheology of Non-Newtonian Fluids: A New Flow Equation for Pseudoplastic Systems," *J. Colloid Sci.*, **20**, 417 (1965).

de Kruif, C. G., E. M. F. van Iersel, A. Vrij, and W. B. Russel, "Hard Sphere Colloidal Dispersions: Viscosity as a Function of Shear Rate and Volume Fraction," *J. Chem. Phys.*, **83**, 4717 (1985).

Hirsch, E., F. Debeauvais, F. Candau, J. Lang, and R. Zana, "Effect of Salinity on the Ultrasonic Absorption and Flow Birefringence of Microemulsions," *J. Physique*, **45**, 257 (1984).

Hoffmann, H., H. Rehage, and A. Rauscher, "Structure and Dynamics of Strongly Interacting Colloids Aggregates in Solution," S. H. Chen et al., eds., Kluwer Academic Publishers (1992).

Hyde, S. T., B. W. Ninham, and T. N. Zemb, "Phase Boundaries for Ternary Microemulsions, Predictions of a Geometric Model," *J. Phys. Chem.*, **93**, 1464 (1989).

Krieger, I. M. Rheometrics Inc., internal report.

Lang, J., A. Djavanbakht, and R. Zana, "Ultrasonic Absorption Study of Microemulsions in Ternary and Pseudoternary Systems," *J. Phys. Chem.*, **84**, 1541 (1980).

Morgan, J., D. H. Napper, G. G. Warr, and S. K. Nicol, "The Kinetics of Recovery of Hexadecyltrimethylammonium Bromide by Flotation," *Langmuir*, **8**, 2124 (1992).

Quemada, D., and D. Langevin, "Rheological Modelling of Microemulsions," *J. Méc. Théor. Appl.*, (Numéro Spécial), 201 (1985).

Radlinska, E. Z., B. W. Ninham, and S. T. Hyde, "Specific Heat is a Useful Indicator of Microstructural Variation in Surfactant Solutions," *Langmuir*, **5**, 1427 (1985).

Rehage, H., and H. Hoffmann, "Rheological Properties of Viscoelastic Surfactant Systems," *J. Phys. Chem.*, **92**, 4712 (1988).

Snabre, P., and G. Porte, "Viscosity of the L_3 Phase in Amphiphilic Systems," *Europhys. Lett.*, **13**, 641 (1992).

Thurston, G. B., J. L. Salager, and R. S. Schechter, "Effects of Salinity on the Viscosity and Birefringence of a Microemulsion System," *J. Colloid Interf. Sci.*, **70**, 517 (1970).

van Blaaderen, A., J. Peetermans, G. Maret, and J. K. G. Dhont, "Long-Time Self-Diffusion of Spherical Colloidal Particles Measured with Fluorescence Recovery after Photobleaching," *J. Chem. Phys.*, **96**, 4591 (1992).

van Megen, W., S. Underwood, R. H. Ottewill, and N. St. J. Williams, "Particle Diffusion in Concentrated Suspensions," *Farad. Discuss. Chem. Soc.*, **83**, 47 (1987).

Winter, H. H., "Viscous Dissipation in Shear Flows of Molten Polymers," *Adv. Heat Transfer*, **13**, 205 (1977).

Manuscript received Nov. 29, 1993, and revision received Feb. 24, 1994.